Cancer Science
Japanese Cancer Association JCA
Open Access

Fhit loss-associated initiation and progression of neoplasia *in vitro*

Jenna R. Karras,[1] Morgan S. Schrock,[1,4] Bahadir Batar,[1,4] Jie Zhang,[2] Krista La Perle,[3] Teresa Druck[1] and Kay Huebner[1]

Departments of [1]Cancer Biology and Genetics; [2]Biomedical Informatics, Ohio State University Wexner Medical Center, Columbus, Ohio; [3]Department of Veterinary Biosciences, College of Veterinary Medicine, Ohio State University, Columbus, Ohio, USA

Key words

Cell transformation, common fragile site, genome instability, kidney cell lines, tumorigenicity

Correspondence

Kay Huebner, Department of Cancer Biology and Genetics, The Biomedical Research Tower, Room 916, 460 W. 12th Avenue, Columbus, OH 43210, USA.
Tel: +1-614-292-4850; Fax: +1-614-688-8675;
E-mail: kay.huebner@osumc.edu

[4]These authors contributed equally to this work.

Funding Information

Ohio State University Comprehensive Cancer Center; The Scientific and Technological Research Council of Turkey; National Cancer Institute (CA120516, CA166905).

Received May 30, 2016; Revised August 5, 2016; Accepted August 9, 2016

Cancer Sci **107** (2016) 1590–1598

doi: 10.1111/cas.13032

The *FHIT* gene, encompassing an active common fragile site, FRA3B, is frequently silenced in preneoplasia and cancer, through gene rearrangement or methylation of regulatory sequences. Silencing of Fhit protein expression causes thymidine kinase 1 downregulation, resulting in dNTP imbalance, and spontaneous replication stress that leads to chromosomal aberrations, allele copy number variations, insertions/deletions, and single-base substitutions. Thus, Fhit, which is reduced in expression in the majority of human cancers, is a genome "caretaker" whose loss initiates genome instability in preneoplastic lesions. To follow the early genetic alterations and functional changes induced by Fhit loss that may recapitulate the neoplastic process *in vitro*, we established epithelial cell lines from kidney tissues of Fhit−/− and +/+ mouse pups early after weaning, and subjected cell cultures to nutritional and carcinogen stress, which +/+ cells did not survive. Through transcriptome profiling and protein expression analysis, we observed changes in the Trp53/p21 and survivin apoptotic pathways in −/− cells, and in expression of proteins involved in epithelial–mesenchymal transition. Some Fhit-deficient cell lines showed anchorage-independent colony formation and increased invasive capacity *in vitro*. Furthermore, cells of stressed Fhit−/− cell lines formed s.c. and metastatic tumors in nude mice. Collectively, we show that Fhit loss and subsequent thymidine kinase 1 inactivation, combined with selective pressures, leads to neoplasia-associated alterations in genes and gene expression patterns *in vitro* and *in vivo*.

Chromosome fragile sites are among the most frequently deleted loci in cancer.[1] The fragile gene, *FHIT*, was identified by the Huebner laboratory[2–4] at a locus that is inactivated in >50% of human cancers.[4,5] *FHIT* locus deletions are among the first genetic changes detected in human preneoplastic lesions.[6,7] Many biological functions are altered by Fhit loss in cancers: decreased apoptosis,[8] increased epithelial–mesenchymal transition (EMT),[9,10] increased resistance to genotoxic agents,[11] altered production of reactive oxygen species,[12] and ongoing genome instability.[13,14] However, the direct mechanisms through which the Fhit protein affects these functions has remained elusive. Lack of a known mechanism of action has slowed general acceptance of a role for Fhit in tumor suppression, despite strong evidence of Fhit association with multiple cancer-associated functions. This skepticism has hindered consideration of Fhit-associated therapeutic targets for the many Fhit-deficient human cancers. For example, the accumulation of genome mutations due to Fhit loss and the ability to stop the accumulation of genome damage by thymidine supplementation[13] hint at possible preneoplasia prevention strategies. In addition, Fhit loss-induced DNA damage creates optimal single-stranded DNA substrates for the APOBEC3B enzyme (a cytidine deaminase that converts cytosines to uracils in single-stranded DNA), illustrating a key role for Fhit loss[15] in hypermutation genotypes observed in most common cancers, a major source of cancer-associated genetic heterogeneity.[16] The APOBEC3B enzyme, which causes hypermutations selectively in Fhit-deficient cells, is likely a critical diagnostic and therapeutic target.[16]

The purpose of the current study was to show that Fhit deficiency supports neoplastic progression. We followed expression changes from establishment, through proliferation in the face of selective pressures, to transformation and nascent neoplastic changes, in epithelial cells from Fhit knockout and wild-type mice. We have observed that Fhit loss is followed by genomic and functional changes in response to selective pressures that allow survival of clonally expanded populations, supporting the conclusion that Fhit loss-induced genome instability enables selection for transformation and neoplastic progression.

Materials and Methods

Ethics statement. Mice were maintained and animal experiments carried out in accord with institutional guidelines established by the Animal Care and Use Committee at Ohio State University (Columbus, OH, USA).

Cell lines and reagents. Mouse kidney cell lines were established by culturing minced mouse kidney tissue from three *Fhit*$^{+/+}$ C57Bl6 (B6 +/+ kd cell lines 1, 2, 3) and three *Fhit*$^{-/-}$ (B6x129SvJ backcross, >99% B6 at genomic level)[17] 5-week-old mice (−/− kd cell lines 2, 3, 4). After emergence of

epithelial cells from minced kidney fragments, cells could be subcultured; these epithelial kidney cell lines did not show an obvious crisis phase but rather grew steadily from first subculturing. Early passage +/+ and −/− kidney lines did not show obvious morphological or proliferation differences (Figs S1,S2). However, late passage −/− kidney lines grew more rapidly than +/+ (Fig. S2). RNA, DNA, and protein were isolated at alternate passages. To establish 7,12-dimethylbenz[a]anthracene (DMBA) survivor (DS) cell lines, late passage (p40) cells were treated with two sequential 24-h, 20-μM DMBA doses, followed by plating and culturing of surviving colonies 8 days post-treatment; +/+ cells did not survive DMBA treatment. To establish nutritionally stressed (NS) cell lines, early passage cells were maintained without replenishing medium for several months, followed by fresh medium and culture of surviving colonies; +/+ cell lines did not survive nutritional stress. The NS cell lines exhibited new morphological features as they transitioned from epithelial to mesenchymal phenotype (Fig. S1). Nutritionally stressed cells also grew to a higher density than +/+ cells (Fig. S2). Some DS and NS cell lines formed colonies in soft agar. Colonies were isolated and replated to establish colony-forming cell lines (Table 1 summarizes cell line characteristics). The mouse cell lines were cultured in MEM with 5% FBS and 100 μg/mL gentamicin. H1299, a human non-small-cell lung carcinoma cell line, was cultured in MEM with 10% FBS and 100 μg/mL gentamicin.

Immunoblots, soft agar growth, and invasion assays. Immunoblots were carried out as described.[13] Antisera[18,19] used and working dilutions are available in Table S1. Soft agar[20] and invasion[21,22] assays were performed as previously described.

Table 1. Derivation of mouse kidney cell lines

Cell line	Derived from	Agar colonies
Fhit +/+		
Subcultured		
+/+ kd1	♀ ms 3451	No
+/+ kd2	♀ ms 3452	No
+/+ kd3	♀ ms 3453	No
Fhit −/−		
Subcultured		
−/− kd2	♀ ms 3454	No
−/− kd3	♂ ms 3455	No
−/− kd4	♂ ms 3456	No
Nutritionally stressed		
NS1	−/− kd3 p3	Yes
NS2	−/− kd2 p1	No
NS3	−/− kd3 p5	Yes
NS4	−/− kd3 p8	No
DMBA survivors		
DS2	−/− kd2 p38	Yes
DS3	−/− kd3 p40	Yes
DS4	−/− kd4 p41	No
Colony forming		
NS1 colony	NS1 p24	Yes
NS3 colony	NS3 p13	Yes
DS2 colony	DS2 p10	Yes
DS3 colony	DS3 p15	Yes

Cell lines were established from culture of single kidneys from three *Fhit*$^{+/+}$ C57Bl6 and three *Fhit*$^{-/-}$ (B6x129SvJ backcross) mice at 5 weeks of age. Nutritionally stressed (NS) cell lines were isolated from early passage −/− kd2 and −/− kd3 lines after maintenance without replenishing medium for 3 months, followed by fresh medium and continued subculture. 7,12-Dimethylbenz[a]anthracene (DMBA) survivor (DS) cell lines were established after treatment with 20 μM DMBA. Colony-forming cell lines were established after excision and plating of soft agar colonies.

***Ras* and *Trp53* sequencing, expression plasmid construction, and transient transfection.** F131L and S151R *Trp53* cDNAs were amplified from NS1 and NS2 cell lines, respectively, using the following conditions: 94°C for 5 min, 30 cycles at 94°C for 30 s, 54°C for 30 s, 68°C for 2 min, and held at 4°C. *Trp53* forward 5′-GCGAAGCTTATGACTGCCATGGAGGAGTCA-3′, and reverse 5′-GCGTCTAGATCAGCCCTGAAGTCATAAGAC-3′ primers were used. Mutant *Trp53* cDNA was cloned into *Hind*III and *Xba*I sites of the pRcCMV vector (Invitrogen, Carlsbad, CA, USA) and recombinant clones were sequenced as previously described.[14] Primers used are available in Table S2.

Microarray expression profiles. Total RNA (+/+kd2 p14, −/− kd3 p48, NS3 colony p13) was isolated using RNeasy Mini Kit (Qiagen, Hilden, Germany). RNA integrity was assessed using the Agilent 2100 Bioanalyzer (Agilent Technologies, Palo Alto, CA, USA). A 100-ng aliquot of total RNA was linearly amplified. Then 5.5 μg cDNA was labeled and fragmented using the GeneChip WT PLUS reagent kit (Affymetrix, Santa Clara, CA, USA) following the manufacturer's instructions. Labeled cDNA targets were hybridized to the Affymetrix GeneChip Mouse Transcriptome Array 1.0 for 16 h at 45°C, with rotation at 60 rpm. Arrays were washed and stained using the Fluidics Station 450 (Ohio State University Medical Center Shared Facility, Columbus, OH, USA) and scanned using the GeneChip Scanner 3000 (Ohio State University Medical Center Shared Facility, Columbus, OH, USA). For gene expression analysis, arrays were normalized using the RMA algorithm in Expression Console and comparisons made in Transcriptome Analysis Console (Affymetrix). Microarray data have been deposited in the NCBI Gene Expression Omnibus (accession # not yet available).

Tumorigenicity and metastasis assays. Athymic nude mice were obtained from the Target Validation Shared Resource of the Ohio State University Comprehensive Cancer Center and maintained on an outbred background. Original breeders (strain#553 and #554) came from the NCI Frederick facility. Fhit$^{+/+}$ (1×10^7) and NS3 colony (1 x 10^7) cells in 100 μL PBS were injected s.c. into the right flank, four mice per cell line, in the first round of injections. Subsequent injections used 5×10^6 (Fhit$^{+/+}$, NS1 colony, NS3 colony, NS3T) cells in a total of 20 mice (six female, 14 male). Mice were monitored twice weekly for tumor formation up to 6 months after inoculation. For assessment of metastatic growth, NS3T cells were injected into seven mice (two female, five male). Briefly, 5×10^6 (or 2×10^6) cells resuspended in 150 μL PBS were tail-vein injected. Mice were monitored twice weekly up to 2 months post-inoculation and sacrificed up to 8 weeks post-injections. Inducible clones B28 and B29 were treated with doxycycline (1 μg/mL) 48 h before harvesting 5×10^6 cells in 150 μL PBS for s.c. injections into the right flank of 18 male mice. Mice received sucrose (30%) or doxycycline water (1.2 mg/mL) beginning 12 days prior to injections with water replacement every 6 days.

Histopathology and immunohistochemistry. Subcutaneous tumors were measured and fixed in 10% neutral buffered formalin; lungs were insufflated with 10% neutral buffered formalin prior to immersion fixation. Tissues were processed by routine methods and embedded in paraffin. Sections (4 μm) were stained with HE or deparaffinized and hydrated for immunohistochemistry, carried out as previously described.[23] Slides were evaluated with an Olympus BX45 light

microscope with attached DP25 digital camera (B & B Microscopes, Ohio State University Veterinary College Shared Facility, Columbus, OH, USA) by a comparative pathologist board certified by the American College of Veterinary Pathologists. The antisera used and the working dilutions are available in Table S1.

Lentiviral vector construction. Wild-type human *FHIT* cDNA was amplified from previously constructed plasmids[24] using the following conditions: 95°C for 3 min, 30 cycles at 98°C for 10 s, 55°C for 15 s, 72°C for 5 s, and held at 4°C. *FHIT* forward 5′-CCCTCGTAAAGAATTCATGTCGTTCAGAT-3′ and reverse 5′- GAGGTGGTCTGGATCCTCACTGAAAGTA-3′ primers were used. The cDNA was cloned into *Eco*RI and *Bam*HI sites of the pLVX-TetOne-Puro vector (Clontech, Mountain View, CA, USA). This vector allows transgene expression by the doxycycline-inducible TRE3G promoter. Transgene expression on doxycycline induction was assessed by immunoblot using anti-Fhit polyclonal serum.

Generation of inducible Fhit transfectants. The recombinant plasmid (pLVX-*FHIT*) was transfected into NS3T mouse kidney cells using Xfect buffer and polymer reagents (Clontech). Mouse kidney cells were plated at a density of 4×10^5 cells per 60-mm dish and cultured in normal growth medium. Transfections were with 5 μg plasmid DNA diluted with 90 μL Xfect buffer before addition of 1.5 μL Xfect polymer. The solution was incubated for 10 min at room temperature. Cells were overlaid with plasmid DNA/polymer solution and incubated for 24 h at 37°C. After 24 h, stable clones were selected in puromycin (2 μg/mL) and tested for doxycycline inducible Fhit expression.

Results

***In vitro* model of Fhit loss-associated neoplastic progression.** To create an *in vitro* model for Fhit-deficient cell transformation, we established mouse kidney epithelial cell lines, three from Fhit+/+ (+/+kd1, +/+kd2, and +/+kd3) and three from Fhit knockout (−/−kd2, −/−kd3, and −/−kd4), post-weaning mice. These cell lines were subcultured through tissue culture passage (p50) and accumulating alterations examined. The initial cell cultures were also used to generate DS and NS survivor cell lines. Fhit+/+ cell lines did not survive these stresses. Thus, there were a total of three Fhit+/+ cell lines and 14 Fhit−/− cell lines, for which different selective pressures were applied (see Table 1 for cell line summary).

Fhit−/− cells show alterations in apoptotic and EMT signal pathways. To follow the evolution of cells from the benign to malignant state *in vitro*, we assessed changes in proteins in signal pathways that are frequently altered in cancers, beginning with the Trp53/p21 and EMT pathways. In assessing the unstressed +/+ and −/− kidney cell lines, a reduction in Trp53 protein expression was observed in late-passage −/−kd3 along with a decrease in its downstream target p21 (Fig. 1a). Trp53/p21 pathway changes were not observed in DS cell lines (Fig. 1b). Striking changes in Trp53/p21 pathway proteins occurred in the NS lines; all four NS lines displayed Trp53 protein expression but lacked p21 expression, suggesting that these cell lines harbor mutated *Trp53* genes, selected for survival of nutritional stress (Fig. 1c). Indeed, absence of p21 expression is due to mutation in the DNA binding domain of the Trp53 protein. All NS lines showed C to G base substitutions, changing a phenylalanine to a leucine at amino acid position 131 (F131L) in NS1, NS3, and NS4 lines, and changing a serine to an arginine at amino acid position 151 (S151R) in NS2 (Fig. S3). Mutations in the Trp53 DNA binding domain can result in faulty transactivation of the *CDKN1A* gene encoding p21 protein. To confirm that p21 protein is downregulated due to Trp53 mutation, we transfected NS lines with wild-type and mutant *Trp53* plasmids to determine if p21 expression could be restored. Re-expression of p21 was observed in both NS1 and NS2 cells that were transfected with wild-type *Trp53*, but not when transfected with F131L or S151R *Trp53* mutants (Fig. 1d). Although DS lines did not exhibit changes in the Trp53/p21 pathway, increased expression of the pro-survival protein, survivin, was observed (Fig. 1e). To discern if Fhit−/− cells have acquired protumorigenic activities, we tracked expression of vimentin, a marker of the mesenchymal phenotype and a hallmark of EMT. All NS lines showed robust expression of vimentin (Fig. 1c), suggesting these cells have undergone EMT and

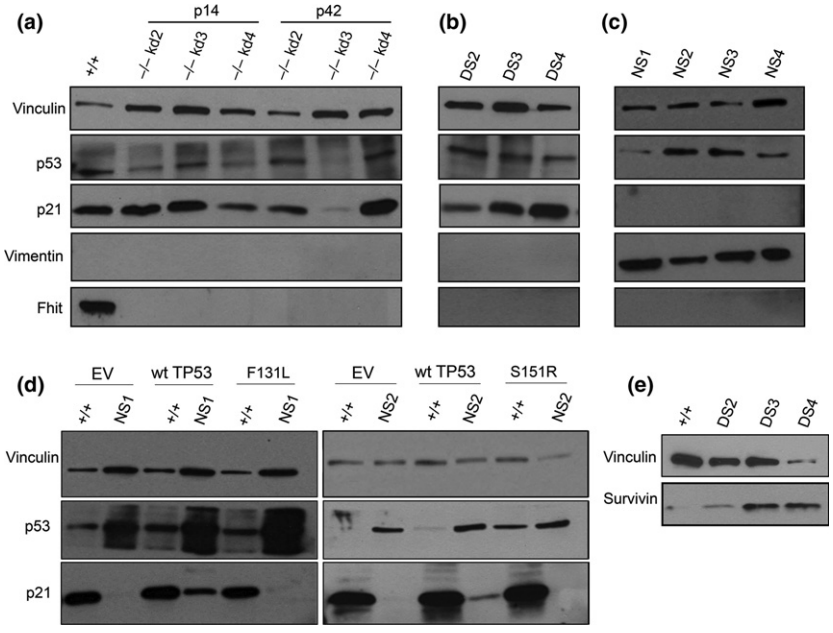

Fig. 1. Fhit−/− mouse kidney cells show signal pathway alterations. Immunoblots of p53, p21, vimentin, Fhit, and vinculin expression in mouse kidney cells with (a) progressive *in vitro* subculture, (b) survival of DMBA (DS), and (c) survival of nutritional stress (NS). Western blot analysis of p21 protein restoration in (d) NS1 and NS2 cell lines by wild-type (wt) p53 overexpression. NS1 and NS2 mouse kidney cells were transfected with control vector (EV), wt or mutant Tp53 (F131L or S151R) expression vector. (e) Immunoblot of survivin expression in DS cells.

possess migratory abilities. Tables S3 and S4 display expression patterns of other proteins tested.

Fhit loss-associated cell transformation. Because protein expression studies provided evidence of *in vitro* transformation in Fhit−/− cells, we compared biological features of +/+ and −/− kd cell lines, by measuring the effect of Fhit deficiency on anchorage-independent growth in soft agar. After 24 days of culture in soft agar, some cells of NS1 and NS3 showed anchorage-independent growth, producing 15 and 13 colonies, respectively (Fig. 2a). Additionally, some cells of DS cell lines DS2 and DS3 formed large colonies (Fig. 2a,b, representative agar colonies at day 24). No colony formation was observed for any of the +/+ and unstressed −/− kd cell lines. Moreover, after collection of agar colonies and propagation, we re-assessed one colony line from each group for colony formation potential. Each new colony cell line showed rapid anchorage-independent growth and formed increased numbers of agar colonies (Fig. 2c). Thus, subpopulations of cells in these lines on exposure to exogenous stress showed anchorage-independent growth and colony formation, characteristics of transformed cells. Western blot analysis showed that Trp53 overexpression and loss of p21 had also occurred in NS1 and NS3 colony cell lines, indicating that the Trp53 missense mutation acquired in NS1 and NS3 was maintained in these colony-forming lines (Fig. 2d). The DS2 colony line expressed normal Trp53/p21 pathway expression, whereas DS3 colony cells had lost Trp53 protein expression, resulting in downregulation of p21 expression, as observed in the −/−kd3 parent cell line. Furthermore, the NS3 colony line showed a dramatic increase in vimentin expression. The NS1 colony line displayed a lower level of vimentin expression; DS2 and DS3 colonies did not express vimentin (Fig. 2d). An invasion assay through a basement matrix-coated membrane was carried out to determine if colony-forming cell lines also showed invasive capacity; the NS3 colony line had significant invasive ability *versus* +/+ controls ($P = 0.01$) (Fig. 2e). The NS1 colony line showed increased invasive potential *versus* a +/+ control cell line, in accord with the low level increase in vimentin expression observed (Fig. 2d,e).

(a)

Cell line	No. total colonies
H1299	>750
+/+ Early	0
+/+ Late	0
–/– Early	0
–/– Late	0
NS1	15
NS2	0
NS3	13
NS4	0
DS2	2
DS3	3
DS4	0

(b)

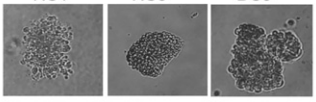

(c)

Cell line	No. total colonies
NS1 colony	>60
NS3 colony	>33
DS2 colony	>15
DS3 colony	>20

(d)

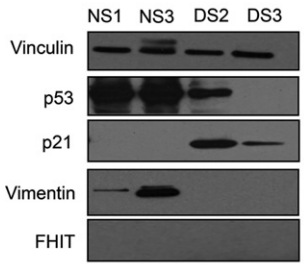

(e)

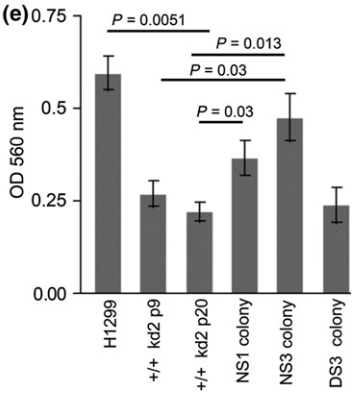

Fig. 2. Transformation-associated Fhit−/− mouse kidney cell features. (a) Anchorage-independent colony formation was observed in four exogenously stressed Fhit−/− cell lines at day 24 in soft agar, but not for Fhit+/+ kd1, 2, 3 nor Fhit−/− kd2, 3, 4 cell lines at early (p4–7) and late (p46–49; p25 for +/+) tissue culture passages, in three independent experiments. (b) Images of colonies; some colonies were excised from agar and propagated in liquid culture. (c) Anchorage-independent growth of newly propagated soft-agar colonies. (d) Western blot analysis of colony-forming cell lines. (e) Invasion assay in triplicate of colony-forming cell lines. Data were analyzed using the Kruskal–Wallis test for multiple comparisons. $P < 0.05$ was considered statistically significant. DS, 7,12-dimethylbenz[a]anthracene survivor; NS, nutritionally stressed.

Classification of genes with altered transcription in a Fhit−/− NS cell line. To further characterize signal pathway alterations that contribute to Fhit loss-supported cellular transformation, we examined signal pathways identified by mRNA expression profiling. Ingenuity Pathway Analysis (IPA) was used to analyze the differentially expressed genes in the *in vitro* invasive NS3 colony cell line, relative to its non-invasive progenitor −/−kd3. Using a significance cut-off of $P < 0.05$ and a fold-change cut-off of 4, there were 432 differentially expressed genes in NS3 colony cells *versus* −/−kd3. An IPA core analysis was carried out to classify this dataset into top biological functions and canonical pathways (Fig. 3a,b), several of which revolve around DNA replication, cell cycle control and DNA repair. An invasion-associated network was constructed to focus on specific genes influencing the invasive phenotype of this cell line (Fig. 3c). Relative to the −/−kd3 parent, the NS3 colony cell line displayed 35-fold downregulation of E-cadherin (*Cdh1*), an epithelial marker, and 55-fold upregulation of vimentin (*Vim*). Upregulation of transcription factors known to induce EMT, such as *Zeb1, Snai2*, and *Foxm1* is also observed in NS3 colony cells.[25–28] Furthermore, genes involved in regulating cell–cell contacts and cell junction integrity are differentially expressed in favor of facilitating the EMT process, confirming that NS3 colony cells are gaining invasive properties. Additionally, a network analysis of DNA damage response-associated genes (Fig. 3d) identified genes important for replication fork progression such as *Top2a, Mcm10, Lig1*, and *Rrm2* that are upregulated, possibly participating in maintaining increased proliferative signaling. *Chek1*, a gene responsible for coordinating the DNA damage response, and DNA double-strand break repair proteins *Brca1* and *Rad51* are also upregulated, suggesting enhanced DNA damage repair in NS3 colony cells. No expression changes were observed for *Myc*, *Raf*, *Mek*, *Erk*, *Erbb2*, *Egfr*, or *Ras*. Sequence analysis of *Kras*, *Hras*, and *Nras* cDNAs from NS cell RNA detected only wild-type sequence at hotspot regions in all NS lines. In the "cyclins/cell cycle regulation" canonical pathway, cyclins *Ccne1*, *Ccne2*, and *Ccnb1* were upregulated 2.78-, 5.29-, and 10.4-fold, respectively, in NS3 colony cells (Fig. 3b), indicating that Fhit loss precedes activation of observed oncogenes in this model system. Collectively, the results suggest that NS3 colony cells acquired signal pathway alterations to meet the challenges of anchorage-independent growth, in accord with the hypothesis that this cell line has undergone malignant transformation.

NS3T cells show tumorigenic and metastatic potential. To assess *in vivo* behavior, we injected the *in vitro* invasive

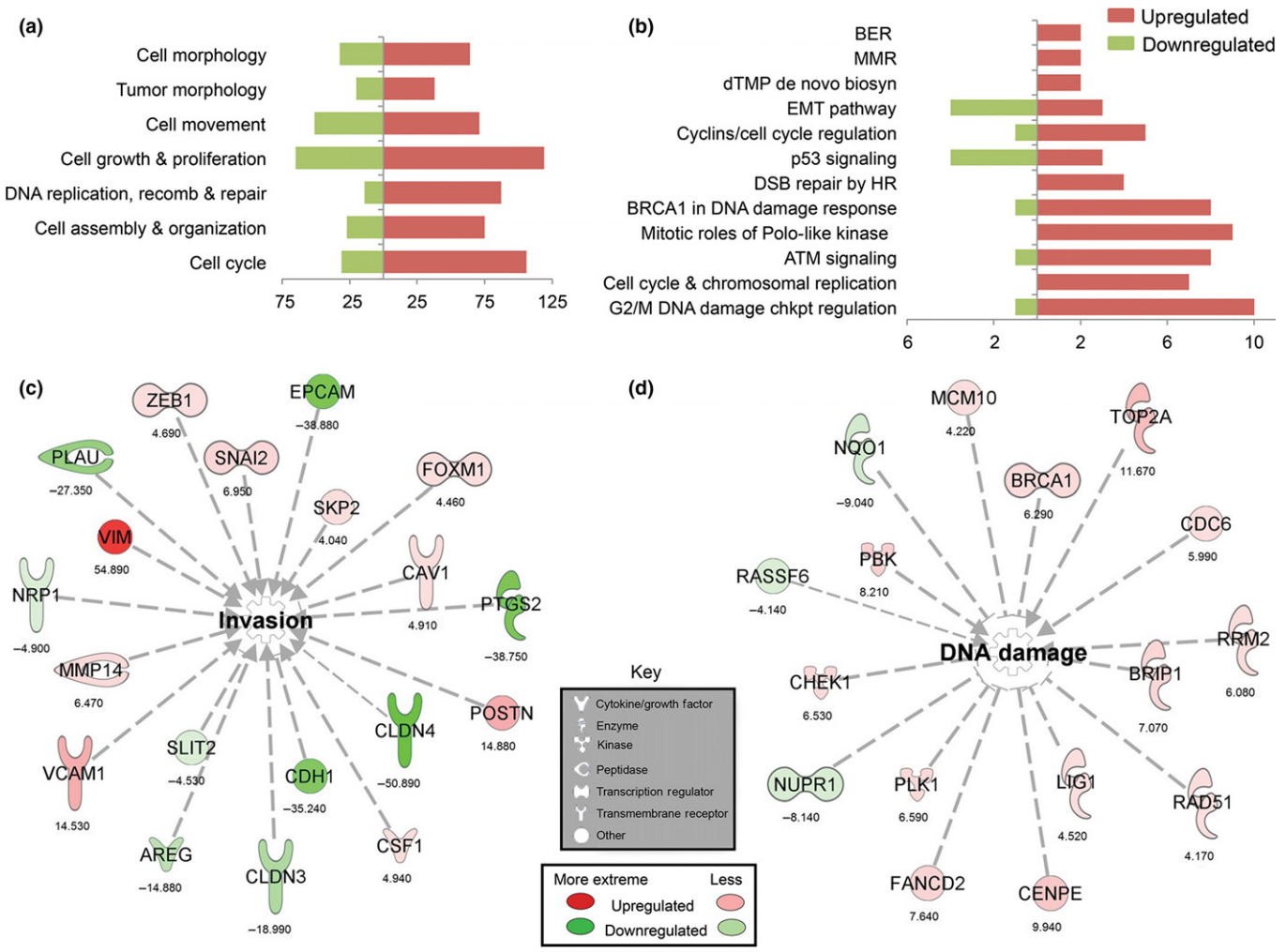

Fig. 3. Classification of genes with altered transcription in NS3 colony cell line *versus* Fhit−/− kd3 p48. Ingenuity Pathway Analysis (IPA) core analysis was used to classify NS3 colony gene expression data into (a) biological functions and (b) canonical pathways. IPA gene networks associated with (c) invasion and (d) DNA damage. Up/downregulated NS3 colony genes are denoted by red and green color, respectively. Fold changes are noted under the nodes. Fisher's exact test was used to determine significant IPA pathway associations.

colony cell lines s.c. into 6-week-old nude mice and observed animals weekly for appearance of tumors. The NS1 colony formed tumors in male mice by day 125. Of two male and two female mice injected, the NS3 colony formed tumors at sites on the shoulder and flank in one male mouse by day 133. Both sites developed sizable tumors by day 151 (flank tumor, 15 × 12 mm; shoulder nodules, 5 × 5 mm and 3 × 5 mm) that showed a mesenchymal spindle cell neoplasm phenotype (Fig. S4). Of four mice injected with +/+kd3 p15, none developed tumors by day 200. NS3 tumors were excised for histopathology, the NS3 flank tumor was cultured *in vitro*, and the tumor outgrowth cell line was designated NS3T. A second round of s.c. injections was performed to determine whether the cultured NS3T cells showed increased tumorigenicity. NS3T p10 and control +/+kd3 p16 cells were injected into flanks of four nude mice each (two females and two males). Both male mice injected with NS3T cells formed tumors within 12 days, with mean tumor size ~100.5 mm^3 by 19 days (Fig. 4a). Neither the female mice nor the +/+kd3-injected mice developed tumors and were sacrificed at day 60. The results suggested that tumor formation was biased towards male mice, possibly because the androgen-receptor is expressed in the NS3 cells as noted in the expression array profile, and the initial cell line was derived from a male mouse kidney; s.c. injections using later passage NS3 colony cells resulted in 100% tumor incidence in female mice. A final round of NS3T cells was injected s.c. into five male nude mice and four of them developed tumors by 10 days (Fig. 4b). See the summary of tumor incidence in Table 2. Two of these s.c. tumors were further characterized for an EMT phenotype by assessment of expression of vimentin, E-cadherin, and cytokeratin using immunohistochemistry. In accord with our transcriptome and Western blot analysis, these tumors were strongly immunoreactive for vimentin and immunonegative for cytokeratin and E-cadherin (Fig. 4c). The metastatic capacity of the NS3T cells was evaluated by tail vein injection in male and female nude mice. Histological examination showed lung micrometastases in 3/5 male and 2/2 female mice. Lung tumors were more abundant (up to five nodules/lung) and larger in male mice sacrificed 43 days post-injection, whereas both female mice showed a small, single neoplastic nodule within one lung lobe when sacrificed 58 days post-injection. Neoplastic cells were

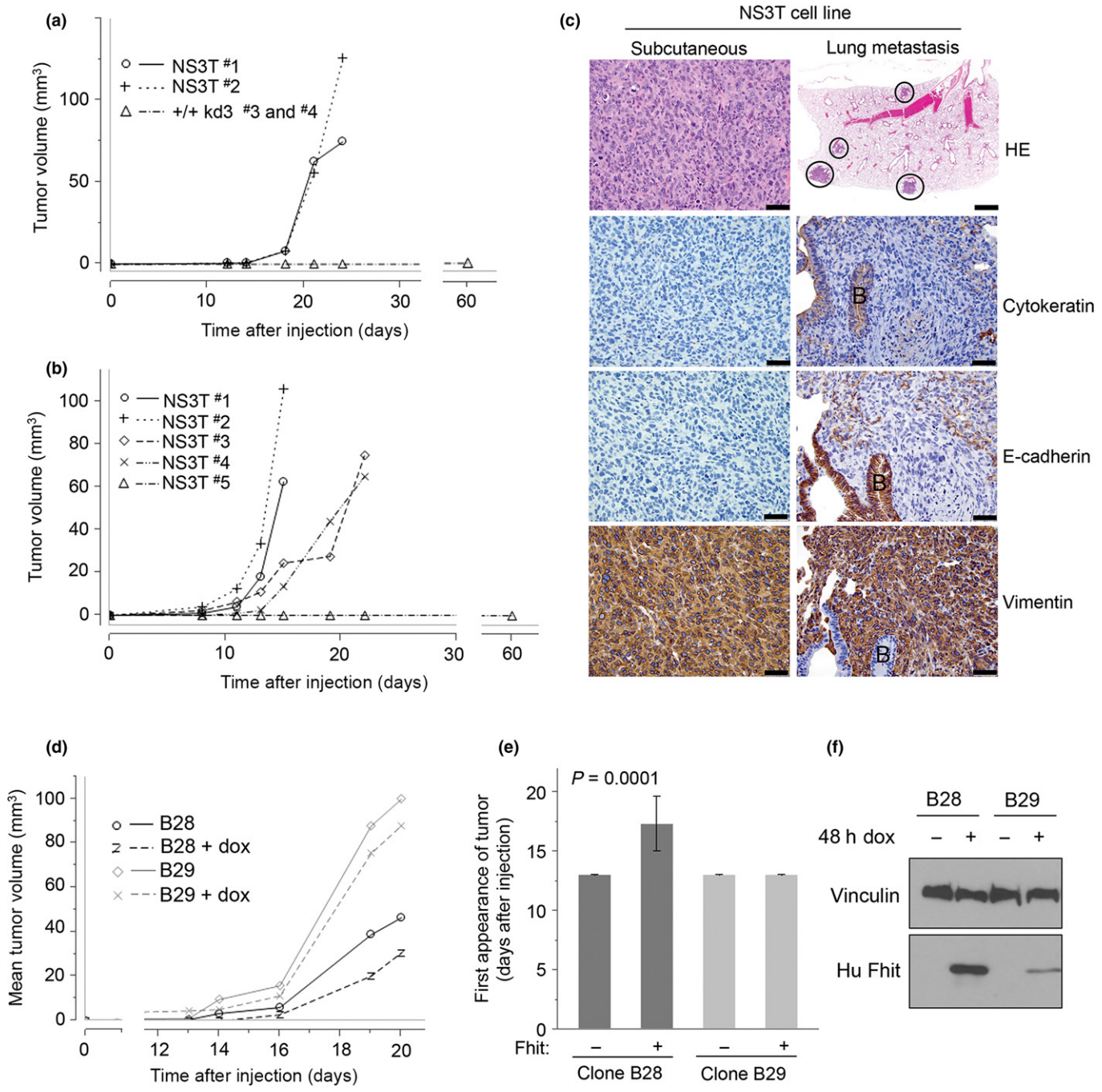

Fig. 4. NS3T mouse kidney cells show tumorigenic and metastatic potential. Tumor growth curves for male nude mice receiving s.c. injection of (a) 5×10^6 NS3T p10 or +/+ kd3 p16 cells or (b) 5×10^6 NS3T p7 cells to the right flank; tumor growth was monitored three times weekly. (c) HE staining and expression of cytokeratin, E-cadherin, and vimentin by immunohistochemical analysis in s.c. tumors and lung metastases (circled). B, bronchiolar epithelium. Scale bar = 50 μm except HE lung metastasis where scale bar = 1 mm. (d) Tumor growth curve for mice receiving s.c. injection of Fhit-inducible NS3T clone B28 or clone B29 cells ± doxycycline (dox). (e) Tumor latency for mice receiving s.c. Fhit-inducible NS3T clones B28 or B29 cells. Mice received doxycycline (1.2 mg/mL) water to induce Fhit expression 12 days before injections and until sacrificed; control mice received sucrose water (30%). (f) Western blot analysis of Fhit expression levels after 48 h doxycycline (1 μg/mL) treatment of NS3T clones B28 and B29 cells. Tumor volumes were calculated using the formula: volume = ½(length × width^2). *T*-test was used to analyze tumor incidence and latency. Error bars depict SD. $P > 0.05$ was considered statistically significant.

distributed within the alveolar parenchyma, around blood vessels and bronchioles, subpleurally or intravascularly. Lung tumors of one male were characterized by immunohistochemistry as performed for primary s.c. tumors. Neoplastic cells in the lung were strongly immunoreactive for vimentin and immunonegative for cytokeratin and E-cadherin, in contrast to normal bronchiolar epithelium (Fig. 4c). Thus, the alterations that occurred *in vitro* contributed to *in vivo* tumorigenicity and metastasis.

Induced Fhit expression delays tumor onset *in vivo*. To confirm that Fhit loss is responsible for tumor initiation *in vitro*, we created two stable NS3T clones, B28 and B29, that were doxycycline-inducible for Fhit expression. For both clones, we observed no differences in soft agar colony growth, *in vitro*

Table 2. Summary of tumorigenicity data in mouse kidney cell lines

Cell line	Sex of host	Route	Days post-injection	Tumor frequency	Comments
NS1 colony	2♂	s.c.	125	2/2	
NS3 colony	2♂	s.c.	200	1/2	
	2♀	s.c.	200	0/2	Early passage (p14)
	2♀	s.c.	200	2/2	Late passage (p27)
NS3T	7♂	s.c.	60	6/7	
	2♀	s.c.	60	0/2	
NS3T	5♂	i.v.	43	3/5	
	2♀	i.v.	58	2/2	
+/+ kd3	3♂	s.c.	125	0/3	Control for NS1 colony injections
+/+ kd3	2♂	s.c.	200	0/2	Control for NS3 colony injections
	2♀	s.c.	200	0/2	Control for NS3 colony injections
+/+ kd3	2♂	s.c.	60	0/2	Control for NS3T injections
	2♀	s.c.	60	0/2	Control for NS3T injections

Initial studies showed that NS3 colony cells did not form tumors in female mice, possibly due to expression of androgen receptor. Thus, NS3 colony tumor incidence was 50% in male mice. Late-passage NS3 colony tumor incidence of 100% in female mice suggests loss of androgen receptor expression. The NS3T tumor incidence was 85% ($P = 0.0109$).

invasive potential, or final tumor volumes *in vivo* between Fhit-deficient and Fhit-induced cells (Fig. 4d). However, clone B28 showed a significantly ($P = 0.0001$) delayed onset of tumor formation in mice induced for Fhit expression by doxycycline water. All B28 control mice developed tumors by day 13, whereas tumors did not start to appear until day 16 in the Fhit-induced mice (Fig. 4e). Clone B29 did not display the same effect on tumor latency following Fhit induction (Fig. 4e). Western blot analysis of the clonal cell lysates revealed that 48-h doxycycline treatment of clone B29 cells caused ~10-fold lower level induction of Fhit protein *versus* clone B28 (Fig. 4f), suggesting that robust Fhit expression is necessary for delaying tumor onset. As there is no selection for retention of the inducible plasmid in the *in vivo* environment, loss of Fhit plasmid and Fhit expression likely explains eventual tumor development by both clones.

Discussion

The translational research world places substantial focus on the late stages of cancer and identification of specific cancer driver genes. But largely because of the extensive genome instability of neoplastic cells underlying the extreme clonal heterogeneity of metastatic cancer, treatment frequently fails due to relapse and therapy resistance. Thus, the idea of concentrating on the biology of premalignancy to advance prevention and early diagnosis is gaining interest. Kensler *et al.*[29] have proposed a Pre-Cancer Genome Atlas initiative for solid tumors of epithelial origin to investigate the molecular alterations associated with premalignant lesions as they progress. Alterations of the *FHIT* gene, straddling a common fragile site, occur in the preneoplastic lesions preceding development of many human cancers.

Point mutations and small insertions/deletions have long been a focus in tumor sequencing; however, recent studies have suggested that genome structural variants, such as deletions and translocations, may play a larger role in cancer progression than previously thought. In 2015, investigators examined the contribution of recurrent structural variations in the progression of pancreatic cancer. Analysis of 24 ductal pancreatic adenocarcinomas revealed that the *FHIT* gene is the second most frequently altered gene, with deletions observed in 50% of pancreatic adenocarcinoma tumors that resulted in reduction of Fhit protein expression.[30] Another study used whole genome sequencing to fully characterize the genomic landscape of gastric and esophageal tumors. Compared to matched normal blood samples, recurrent deletions at the *FHIT* locus were identified in 46% of tumors.[31] Our laboratory has shown that such alterations at the *FHIT* locus can lead to loss of Fhit protein expression, causing mild replication stress through TK1 down-regulation and subsequent dNTP imbalance.[13]

The current study followed *in vitro* cellular alterations associated with Fhit absence to illustrate that loss of Fhit genome caretaker function supports *in vitro* tumorigenic progression. We showed that Fhit loss provides a survival and expansion advantage when selective pressures are applied, enabling selection for preneoplastic properties. As proof that Fhit loss provides a survival advantage, all three Fhit+/+ cell lines did not survive exogenous stress, whereas all Fhit−/− cell lines had surviving colonies, revealing that Fhit loss-associated genome instability allows a fraction of Fhit−/− cells to survive these stresses, even at early tissue culture passages. Furthermore, in contrast to Fhit+/+ cells, we showed that loss of Fhit, combined with stressful exposures, leads to alterations in apoptotic and EMT signaling pathways and oncogene activation. These alterations allow for transformation, selective clonal expansion, and development of invasive properties *in vitro* and tumor formation and metastasis *in vivo*. Finally, induction of exogenous wild-type Fhit protein delayed the onset of tumor formation *in vivo*. The documentation of frequent *FHIT* allele losses in precancerous lesions, in combination with our demonstration that loss of Fhit expression supports preneoplastic and neoplastic clonal expansion, reveals Fhit loss as a driver of neoplastic progression. The findings support an undertaking to search for *in vivo* methods to prevent replication stress at *FHIT* and other fragile loci, or to prevent the consequences of Fhit loss. We have shown that *in vitro* thymidine supplementation of Fhit−/− cells prevents ongoing genome instability, implying that inactivation of the Fhit–TK1 pathway underlies the generation of genome instability that allows clonal expansion.[13] Although many studies have shown that dNTP pool imbalances cause replication stress and mutations leading to tumorigenesis,[32–34] it is not known whether *in vivo* thymidine supplementation would be a feasible prevention approach. Testing of thymidine supplementation to support genome stability may be an important avenue for intensive

preclinical research and may inspire additional approaches to inhibit genome instability.

In summary, this study demonstrates that Fhit-deficient cells are more likely to acquire cancer-promoting mutations. Through selective pressures to survive, activating mutations in oncogenes or inactivating mutations in tumor suppressor genes expedites the cellular transformation process. We conclude that in preneoplastic lesions of human tissues, losing Fhit provides a selective advantage for transformation and cancer progression. The significance of Fhit loss as an alteration that lies at the core of cancer initiation and progression should be exploited as a prevention or therapeutic target due to its relevance in >50% of human cancers.

Acknowledgments

This work was supported by: Ohio State University Comprehensive Cancer Center (OSUCCC) Pelotonia Graduate Student (to M.S.S.) and Postdoctoral (to B.B.) Fellowships; a fellowship from The Scientific and Technological Research Council of Turkey (TUBITAK to B.B.); and NCI grants CA120516 (to K.H.) and CA166905 (J.R.K.-PI: C.M. Croce). We acknowledge The Target Validation Shared Resource at OSUCCC for nude mice, the Genomics and Campus Microscopy and Imaging Facility, and Mouse Phenotyping shared resources.

Disclosure Statement

The authors have no conflict of interest.

References

1 Bignell GR, Greenman CD, Davies H *et al.* Signatures of mutation and selection in the cancer genome. *Nature* 2010; **463**: 893–8.
2 Ohta M, Inoue H, Cottecelli MG *et al.* The FHIT gene, spanning the chromosome 3p14.2 fragile site and renal carcinoma-associated t(3;8) breakpoint, is abnormal in digest tract cancers. *Cell* 1996; **84**: 587–97.
3 Karras JR, Paisie CA, Huebner K. Replicative stress and the FHIT gene: roles in tumor suppression, genome stability and prevention of carcinogenesis. *Cancers (Basel)* 2014; **6**: 1208–19.
4 Pichiorri F, Palumbo T, Suh SS *et al.* Fhit tumor suppressor: guardian of the preneoplastic genome. *Future Oncol* 2008; **4**: 815–24.
5 Waters CE, Saldivar JC, Hosseini SA *et al.* The FHIT gene product: tumor suppressor and genome "caretaker". *Cell Mol Life Sci* 2014; **71**: 4577–87.
6 Gorgoulis VG, Vassiliou LV, Karakaidos P *et al.* Activation of the DNA damage checkpoint and genomic instability in human precancerous lesions. *Nature* 2005; **434**: 907–13.
7 Bartkova J, Horejsi Z, Koed K *et al.* DNA damage response as a candidate anti-cancer barrier in early human tumorigenesis. *Nature* 2005; **434**: 864–70.
8 Sard L, Accornero P, Tornielli S *et al.* The tumor-suppressor gene FHIT is involved in the regulation of apoptosis and in cell cycle control. *Proc Natl Acad Sci USA* 1999; **96**: 8489–92.
9 Joannes A, Grelet S, Duca L *et al.* Fhit regulates EMT targets through an EGFR/Src/ERK/Slug signaling axis in human bronchial cells. *Mol Cancer Res* 2014; **12**: 775–83.
10 Suh SS, Yoo JY, Cui R *et al.* FHIT suppresses epithelial-mesenchymal transition (EMT) and metastasis in lung cancer through modulation of microRNAs. *PLoS Genet* 2014; **10**: e1004652.
11 Ottey M, Han SY, Druck T *et al.* Fhit-deficient normal and cancer cells are mitomycin C and UVC resistant. *Br J Cancer* 2004; **91**: 1669–77.
12 Okumura H, Ishii H, Pichiorri F *et al.* Fragile gene product, Fhit, in oxidative and replicative stress responses. *Cancer Sci* 2009; **100**: 1145–50.
13 Saldivar JC, Miuma S, Bene J *et al.* Initiation of genome instability and preneoplastic processes through loss of Fhit expression. *PLoS Genet* 2012; **8**: e1003077.
14 Miuma S, Saldivar JC, Karras JR *et al.* Fhit deficiency-induced global genome instability promotes mutation and clonal expansion. *PLoS ONE* 2013; **8**: e80730.
15 Waters CE, Saldivar JC, Amin ZA *et al.* FHIT loss-induced DNA damage creates optimal APOBEC substrates: insights into APOBEC-mediated mutagenesis. *Oncotarget* 2015; **6**: 3409–19.
16 Burns MB, Leonard B, Harris RS. APOBEC3B: pathological consequences of an innate immune DNA mutator. *Biomed J* 2015; **38**: 102–10.
17 Paisie CA, Schrock MS, Karras JR *et al.* Exome-wide single-base substitutions in tissues and derived cell lines of the constitutive Fhit knockout mouse. *Cancer Sci* 2016; **107**: 528–35.
18 Fong LY, Fidanza V, Zanesi N *et al.* Muir-Torre-like syndrome in Fhit-deficient mice. *Proc Natl Acad Sci USA* 2000; **97**: 4742–7.
19 Guler G, Uner A, Guler N *et al.* The fragile genes FHIT and WWOX are inactivated coordinately in invasive breast carcinoma. *Cancer* 2004; **100**: 1605–14.
20 Winn RA, Van Scoyk M, Hammond M *et al.* Antitumorigenic effect of Wnt 7a and Fzd 9 in non-small cell lung cancer cells is mediated through ERK-5-dependent activation of peroxisome proliferator-activated receptor gamma. *J Biol Chem* 2006; **281**: 26943–50.
21 Xing X, Zhang L, Wen X *et al.* PP242 suppresses cell proliferation, metastasis, and angiogenesis of gastric cancer through inhibition of the PI3K/AKT/mTOR pathway. *Anticancer Drugs* 2014; **25**: 1129–40.
22 Iseri OD, Sahin FI, Terzi YK *et al.* beta-Adrenoreceptor antagonists reduce cancer cell proliferation, invasion, and migration. *Pharm Biol* 2014; **52**: 1374–81.
23 Guler G, Balci S, Costinean S *et al.* Stem cell-related markers in primary breast cancers and associated metastatic lesions. *Mod Pathol* 2012; **25**: 949–55.
24 Siprashvili Z, Sozzi G, Barnes LD *et al.* Replacement of Fhit in cancer cells suppresses umorigenicity. *Proc Natl Acad Sci USA* 1997; **94**: 13771–6.
25 De Craene B, Berx G. Regulatory networks defining EMT during cancer initiation and progression. *Nat Rev Cancer* 2013; **13**: 97–110.
26 Alves CC, Carneiro F, Hoefler H *et al.* Role of the epithelial–mesenchymal transition regulator Slug in primary human cancers. *Front Biosci* 2009; **14**: 3035–50.
27 Spaderna S, Schmalhofer O, Wahlbuhl M *et al.* The transcriptional repressor ZEB1 promotes metastasis and loss of cell polarity in cancer. *Cancer Res* 2008; **68**: 537–44.
28 Bao B, Wang Z, Ali S *et al.* Over-expression of FoxM1 leads to epithelial-mesenchymal transition and cancer stem cell phenotype in pancreatic cancer cells. *J Cell Biochem* 2011; **112**: 2296–306.
29 Kensler TW, Spira A, Garber JE *et al.* Transforming cancer prevention through precision medicine and immune-oncology. *Cancer Prev Res (Phila)* 2016; **9**: 2–10.
30 Murphy SJ, Hart SN, Halling GC *et al.* Integrated genomic analysis of pancreatic ductal adenocarcinomas reveals genomic rearrangement events as significant drivers of disease. *Cancer Res* 2016; **76**: 749–61.
31 Hu N, Kadota M, Liu H *et al.* Genomic landscape of somatic alterations in esophageal squamous cell carcinoma and gastric cancer. *Cancer Res* 2016; **76**: 1714–1723; e-pub ahead of print 8 February 2016; doi: 10.1158/0008-5472.
32 Bester AC, Roniger M, Oren YS *et al.* Nucleotide deficiency promotes genomic instability in early stages of cancer development. *Cell* 2011; **145**: 435–46.
33 Chabosseau P, Buhagiar-Labarchede G, Onclercg-Delic R *et al.* Pyrimidine pool imbalance induced by BLM helicase deficiency contributes to genetic instability in Bloom syndrome. *Nat Commun* 2011; **2**: 368.
34 Kumar D, Abdulovic AL, Viberg J *et al.* Mechanisms of mutagenesis in vivo due to imbalanced dNTP pools. *Nucleic Acids Res* 2011; **39**: 1360–71.

Supporting Information

Additional Supporting Information may be found online in the supporting information tab for this article:

Table S1. Antisera used, dilutions and applications.

Table S2. Primers used for gene amplification. Note: *Trp53* and *Nras* coding regions were amplified and sequenced from cDNA; genomic DNA was used to amplify and sequence exons 1, 2, and 3 of *Kras* and exons 1, 2 of *Hras*.

Table S3. Protein expression changes in Fhit−/− and +/+ kidney cell lines. Expression analysis of proteins at early (p3–16) and late (p40–50) tissue culture passages. +++, Very strongly expressed; ++, strongly expressed; +, moderately expressed; +/−, faint expression; −, absent.

Table S4. Protein expression in Fhit−/− DMBA survivor (DS), nutritionally stressed (NS), and colony-forming cell lines. +++, Very strongly expressed; ++, strongly expressed; +, moderately expressed; +/−, faint expression; −, absent.

Fig. S1. Photographs of +/+ and −/− mouse kidney cell lines. Cells were examined by light and phase-contrast microscopy. Classic epithelial morphology is observed in +/+ and −/− lines at early and late passages. NS lines and NS3T show a mesenchymal phenotype where cells are less cuboidal and more elongated in shape.

Fig. S2. Proliferation assay of +/+ and −/− mouse kidney cell lines. Cells (1×10^5) of each cell line were plated in duplicate. Cells were counted using TC20 Automated Cell Counter (Bio-Rad) at 4, 8, 12, 24, and 48 h after plating. Error bars indicate SE at each time point for three independent experiments. Growth kinetics for early and late passage wt kd3 cell lines were not significantly different (48 h; $P = 0.07$). At 48 h, the −/− kd3 p11 cells showed growth kinetics similar to wt cells ($P = 0.241$); however, a significant increase in growth kinetics of −/−kd3 p53 was observed ($P = 0.014$). NS, not significant.

Fig. S3. Chromatogram of *Trp53* sequences in NS cell lines. Heterozygous C>G mutation at amino acid position 151 in NS2 cells, changing a serine to an arginine; homozygous C>G mutation at amino acid position 131 for NS1, NS3, and NS4 cells, changing a phenylalanine to a leucine.

Fig. S4. Mesenchymal spindle cell neoplasm phenotype of NS3 colony tumors. NS3 colony cells were injected s.c. into the flank and shoulder of one male nude mouse. Both sites developed tumors that show a histological phenotype consistent with a mesenchymal spindle cell neoplasm. All masses are unencapsulated and composed of mesenchymal spindle cells on a fine fibrovascular, with distinct collagen fibrils between individual neoplastic cells. Multinucleated cells are also prominent.